OMICS Journal of Radiology
ISSN: 2167-7964

Zhang et al., OMICS J Radiology 2013, 2:8
DOI: 10.4172/2167-7964.1000150

Research Article Open Access

A Manual, Semi-Automated and Automated ROI Study of fMRI Hemodynamic Response in the Caudate Nucleus

Jing Zhang[1]*, Erin A Hazlett[2], King-Wai Chu[2] and Monte S Buchsbaum[2]

[1]*Department of Bioinformatics, School of Biomedical Engineering, Capital Medical University, Beijing 100069, PR China*
[2]*Department of Psychiatry, Mount Sinai School of Medicine, New York, NY 10029, USA*

Abstract

This study investigated abnormalities of fMRI Hemodynamic Response (HR) in the caudate nucleus in schizophrenia with manual, semi-automated and automated approaches. The three approaches were applied to generate the Region of Interest (ROI) and extract fMRI HR from the ROI. Compared with controls, less activation with delayed fMRI HR in the caudate were observed in the patient group. High correlations of the AUC were found between the manual and semi-automated ROI approaches, but not between the manual and the automated ROI approach. In addition, the location and size of the automated box ROI are critical for the fMRI HR curve extracted. The abnormal fMRI hemodynamic response in the caudate in the patient group may suggest functional deficits in the frontal-striatal-thalamic circuit in schizophrenia. To speed up fMRI data analysis in anatomical ROI, the semi-automated approach may be used as an alternative to the manual approach in detecting fMRI experimental effect.

Keywords: Regions of interest; fMRI; Hemodynamic response; Area under the curve

Introduction

Since Blood-Oxygen-Level Dependent (BOLD) Functional Magnetic Resonance Imaging (fMRI) was introduced [1], BOLD fMRI has been widely used to investigate the human brain *in vivo* by measuring regional cerebral blood flow and revealing the underlying neural activity. Recent advances in fMRI allow researchers to study psychiatric disorders with better spatial and temporal resolutions. Consequently, there is growing interests in applying fMRI to psychiatric research [2-9]. fMRI and other functional neuroimaging techniques have demonstrated that resting neural activity and activation during a variety of cognitive tasks are abnormal in schizophrenia [10] in brain regions such as the prefrontal and temporal cortex, cingulate gyrus, hippocampus, striatum, thalamus and the cerebellum [5,11]. Reduced and delayed hemodynamic responses in schizophrenia has been detected by fMRI [11,12] and there is also evidence that people genetically at risk of schizophrenia have changed spatial patterns of brain activity in the face of apparently normal cognition [13,14]. Furthermore, Whalley et al. [15] reported that fMRI technique may identify people in whom the first symptoms are beginning to emerge [14] which suggest that early treatment may be important.

The caudate nucleus is a sub-cortical region in the striatum that plays an important role in voluntary movement control, memory and learning. It is linked to the frontal cortex and the thalamus through the frontal-striatal-thalamic circuit. Compared with controls, reduced activations in the caudate nucleus in schizophrenia have been reported by a number of fMRI studies in tasks such as prepulse inhibition startle, working memory and learning [4,12,15,16]. Previous studies also indicate that striatal abnormalities occurred in schizophrenia patients and unaffected siblings [17].

In order to detect regional BOLD signal changes in the brain, fMRI time course is usually extracted from Regions of Interest (ROIs). One common fMRI ROI analysis is to create small ROIs at the peaks of activation clusters. Another approach is to specify a set of anatomical ROIs (regardless of activation or not) and perform statistical analysis on the fMRI data across these regions [18]. Manual delineation of ROIs is relatively accurate for ROIs such as sub-cortical structures, but manually tracing ROI is time consuming, hard for large sample study and often lack of reproducibility across different tracers or laboratories. In practice, since there can be substantial variability between individuals in anatomy, it requires caution whether the ROI analysis is based on single-subject anatomical atlas or the Talairach atlas [18]. In order to minimize manual intervention, some researchers have suggested other analysis methods such as using automated program to label brain regions [19,20]. These automated methods are simple and quick, but limited by the potential inaccuracy introduced by spatial normalization to a brain template. An alternative is semi-automated approach which combines manual and automatic approaches, e.g., SABRE [21] is based on user defined landmarks and regions of interest defined by Dade et al. [22]. In addition, semi-automated tracing software such as SNAP can speed up the tracing of ROIs [23].

In this study, we considered the caudate nucleus as the ROI and investigated the fMRI hemodynamic response in the caudate nucleus in schizophrenia with 3 approaches: (1) manual delineation of the ROI, (2) semi-automated delineation that traced the caudate with the SNAP program on the MNI (Montreal Neurological Institute) brain, and (3) automated delineation of the ROI.

Materials and Methods

fMRI data

The fMRI data were acquired from a startle study with 13 un-medicated schizophrenia patients (3 females, 10 males; mean+SD age: 38.5+15.9 years) and 13 healthy controls (5 females, 8 males; mean ± SD age: 35.9 ± 11.7 years) whom were scanned on a head-

***Corresponding author:** Jing Zhang, School of Biomedical Engineering, Capital Medical University Beijing 100069, PR China, Tel: +86-10-8391-1363; Fax: +86-10-8391-1544; E-mail: jzhang0000@163.com

Received September 15, 2013; **Accepted** October 15, 2013; **Published** October 20, 2013

Citation: Zhang J, Hazlett EA, Chu KW, Buchsbaum MS (2013) A Manual, Semi-Automated and Automated ROI Study of fMRI Hemodynamic Response in the Caudate Nucleus. OMICS J Radiology 2: 150. doi:10.4172/2167-7964.1000150

dedicated Siemens Allegra 3.0-Tesla MRI scanner at the Mount Sinai Medical Center. This study was approved by the IRB at the Mount Sinai School of Medicine. There was no significant difference in age and sex between the patient and control groups. The fMRI acquisition occurred during an event-related attention-to-prepulse paradigm where the major stimuli were the attended and ignored tones followed by a startle sound. Details of the paradigm are described by Volz et al. [16]. The BOLD imaging was performed using a gradient echo planar (GE-EPI) sequence (28 axial slices, 3 mm thick, skip=1 mm, TR=2s, TE=40 ms, flip angle=90°, FOV=210, matrix=64×64) and the participants underwent six 4.5-min BOLD fMRI scan blocks.

For structural images, a T1-weighted MP-RAGE (Magnetization Prepared Rapid Gradient Echo) was used (208 slices with slice thickness=0.82 mm, matrix size=256×256×208, FOV=21 CM, TR=2500 ms, TE=4.38 ms, TI=1100 ms and an 8° flip angle FLASH acquisition).

Data processing

The following pre-processing was performed on the fMRI data with tools provided by FSL software [24]. Motion correction with FSL.MCFLIRT; brain extraction with FSL.BET; mean-based intensity normalization and high-pass temporal filtering (FSL temporal filter, sigma=100.0s).

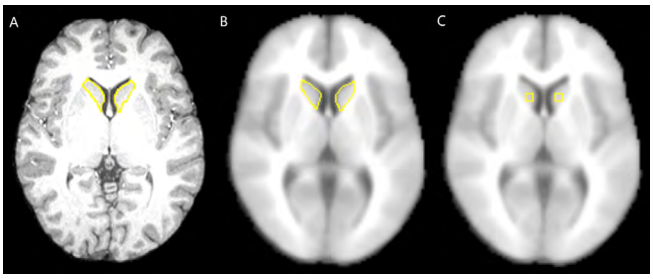

Figure 1: Illustration of manual, semi-automated and automated ROI delineation approaches.

A. Manual (hand-traced) ROI (traced on ACPC-positioned MRI) approach (applied to coregistered fMRI).
B. Semi-automated ROI (traced on the MNI brain with SNAP) approach.
C. Automated box-shape ROI (specified in the Talariach space) approach.

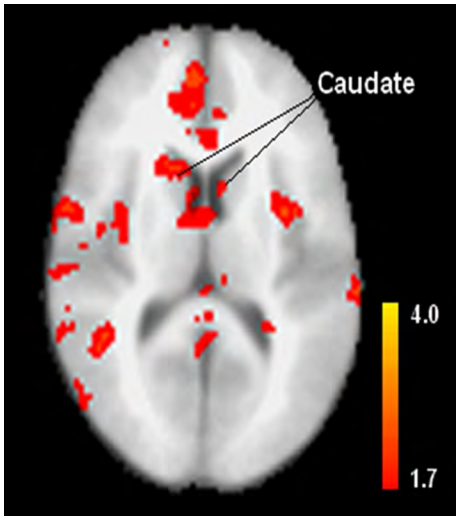

Figure 2: SPM of the contrast of fMRI activation between controls and patients during the attended tone.

The SPM contrast is formed by subtracting fMRI activation of patients from that of controls (Z>1.7, p<0.05, uncorrected). Red clusters in the caudate indicate the higher fMRI activation in controls than patients.

fMRI ROI analysis were performed in 3 ways: (1) manual ROI approach: caudate ROI was traced on anterior-posterior commissure (ACPC)-positioned individual MRI and applied to the coregistered fMRI images (Figure 1A); (2) semi-automated ROI approach: ROI was traced on the MNI (Montreal Neurological Institute) template with the SNAP program (a semi-automated tracing tool) and applied to each subject's fMRI image that was normalized to the MNI (Montreal Neurological Institute) brain template (Figure 1B); and (3) automated ROI approach: fMRI data were normalized to MNI brain template and stereotactic box-shape ROIs were specified with Talairach coordinates (Figure 1C).

To understand the impact of location and size of the automated ROI, pairs of box-based ROIs were placed on the caudate: with center (12, 12, 12), (16, 12, 12), (16, 16, 12), (12, 8, 12) (in Talairach coordinates) for the right caudate; and (-12, 12, 12), (-16, 12, 12), (-16, 16, 12), (-12, 8, 12) for the left caudate respectively. For simplicity, the 4 pairs of box-based ROIs are addressed as x12y12, x16y12, x16y16 and x12y8. Three sizes (3×3×3, 5×5×5, 7×7×7) of these box-shape ROIs were defined with Talairach coordinates to see the impact of automated ROI size. The box-based ROIs were automatically generated by the software developed in the Neuroscience PET Laboratory at the Mt. Sinai Medical Center.

The details on how hand-traced ROIs were generated were described in fMRI study [16]. Briefly, the ROIs were traced on the structural MRI and applied to the co-registered fMRI data. The fMRI hemodynamic response time course extracted from these ROIs were averaged over all voxels within the ROIs across all trials.

Statistical analysis

Analysis of Variance (ANOVA) was performed on the time course data extracted from the ROIs. The set up of mixed-design ANOVA was: Group×Condition (attended tone, ignored tone)×Time. Multivariate Wilks and Greenhouse-Geisser epsilon corrections were used to adjust repeated-measures F values on the mean of each ROI. Hemodynamic response curves were drawn under each condition.

The Area Under the Curve (AUC) of hemodynamic response was used to measure the performance of different ROIs. AUC was calculated in 4 ways: (1) adding only positive points in the BOLD response curve; (2) adding the root mean square of the points in the curve; (3) adding all points in the curve; (4) adding the absolute values of points in the curve.

Correlations between box-based ROI and hand-traced ROI were computed and t-test between patients and controls was performed on the AUC results.

Results

The Statistical Parametric Map (SPM) in Figure 2 is a comparison between patients and controls. It reveals that schizophrenia patients had less activation in the caudate than controls, which is partially reflected in Table 1.

When comparing the two groups with the Area Under the Curve (AUC) measures, Table 2 indicates that patients have smaller AUC than controls using the manual (significant at 1-tailed *t*-test, p=0.091), semi-automated (not significant, p=0.123), and automated ROI (with size 3×3×3, 5×5×5 and 7×7×7 boxes centered at (± 12,12,12), significant

Condition	Measure	Group Mean		*t*-value	p
		Controls	Patients		
Attend	Mean	0.14	-0.17	1.47	0.155
	Min	-3.05	-2.90	-0.77	0.448
	Max	3.18	2.60	2.76	**0.011**
Attend -Ignore	Mean	0.14	0.04	0.40	0.694
	Min	-2.83	-2.61	-0.94	0.359
	Max	3.05	2.63	1.40	0.176

Mean: averaged z-value in the caudate; Min: minimal z-value in the caudate; Max: maximal z-value in the caudate.

Table 1: t-test between patients and controls of Z-values in the caudate in SPM.

Condition	Measure	Manual	Semi-Auto	Auto (Size:7 center (± 12, 12, 12))
Attend	Positive AUC (Pos_AUC)	-0.23	-0.05	-0.54
	Root mean square (RMS)	-0.15	0.06	-0.06
	All AUC (All_AUC)	-0.31	-0.16	-0.58
	Absolute AUC (Abs_AUC)	-0.04	0.10	0.13
Attend -Ignore	Positive AUC (Pos_AUC)	-0.26	-0.03	-0.51
	Root mean square (RMS)	**-0.72**	-0.64	**-0.89**
	All AUC (All_AUC)	-0.07	-0.23	-0.07
	Absolute AUC (Abs_AUC)	0.60	0.52	**0.82**

AUC: area under the hemodynamic response curve; Manual: hand-traced ROI; Semi-auto: semi-automated ROI; Auto: automated ROI; attend: during the attended tone; attend - ignore: difference between the attended and ignored tone. Mean1: mean of controls; Mean2: mean of patients; Bold numbers: Significant 1-tailed t-test between patients and controls.

Table 2: Comparison between manual, semi-automated and automated ROI approaches (in effect sizes).

Condition	Measure	Semi-auto	Size 3 box (± 12,12,12)	Size 5 box (± 12,12,12)	Size 7 box (± 12,12,12)	Size7 box (± 12,12,4)
Attend	Positive AUC	.8653 p=.000	.3534 p=.077	.3700 p=.063	.4167 p=.034	.2334 p=.251
	Root mean square	.8068 p=.000	.5625 p=.003	.5848 p=.002	.6219 p=.001	.4979 p=.010
	All AUC	.8844 p=.000	.1646 p=.422	.1761 p=.390	.2125 p=.297	.0687 p=.739
	Absolute AUC	.8057 p=.000	.4333 p=.027	.4580 p=.019	.5018 p=.009	.4072 p=.039
Attend -Ignore	Positive AUC	.9017 p=.000	.6194 p=.001	.6408 p=.000	.6779 p=.000	.2067 p=.311
	Root mean square	.9203 p=.000	.8260 p=.000	.8352 p=.000	.8584 p=.000	.6901 p=.000
	All AUC	.9627 p=.000	.8542 p=.000	.8629 p=.000	.8781 p=.000	.6473 p=.000
	Absolute AUC	.9466 p=.000	.8064 p=.000	.8153 p=.000	.8431 p=.000	.7205 p=.000

AUC: area under the fMRI HR curve; AUC measures 1-8 correspond to the measures 1-8 in Table 1. attend: during the attended tone; pos: count positive points only; auc: compute area under the curve; abs: count absolute value. Diff: i.e., attend-ignore, AUC difference of attended – ignored tone. Size 3, 5, 7: automated approach with 3x3, 5x5, 7x7 box ROI centered at (±12, 12, 12); Significance 2-tailed t-test at p<0.05.

Table 3: Correlations between manual and semi-automated, manual and automated ROI approaches (box size 3x3x3, 5x5x5 and 7x7x7 voxels).

at 1-tailed t-test, p=0.077, 0.063 and 0.053) approaches measured by Root Mean Square (RMS). The results of effect size are consistent with t-test results (Table 2).

The correlations between manual and semi-automated, manual and automated ROI approaches (included size 3×3×3, 5×5×5 and 7×7×7 boxes) are listed in Table 3. One can see that the correlation of area under the hemodynamic response curve (AUC) between manual and semi-automated approaches is significantly high (R=0.81-0.96), while the correlations of AUC between manual and automated ROI approaches are relatively low. Among the 4 box ROIs compared (size 3×3×4, 5×5×5 and 7×7×7 voxel-boxes are at the same z level, and size 7×7×7 voxel-box is at another z level), the box with size 7×7×7 voxels

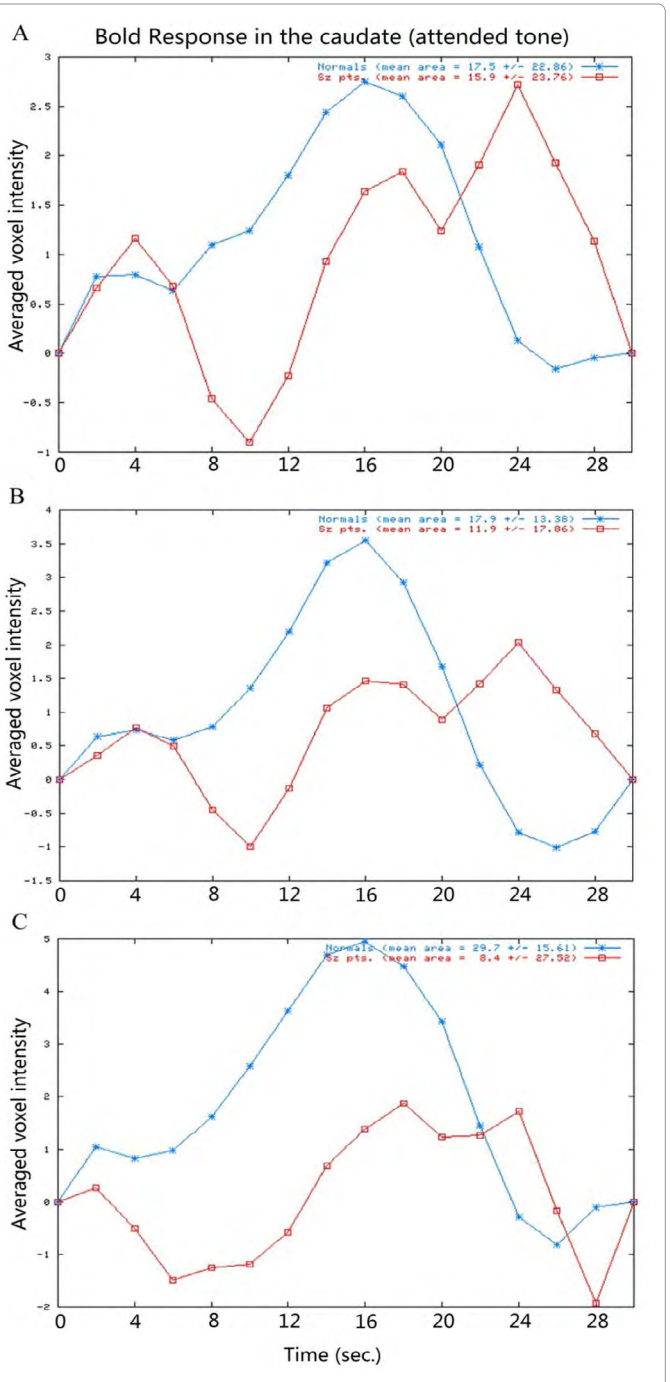

Figure 3: (Hemodynamic response curves during the attended tone extracted from the caudate ROI traced with manual, semi-automated and automated approaches.

A. Hemodynamic response curves extracted from manually traced caudate

B. Hemodynamic response curves extracted from semi-automated ROI traced with SNAP program

C. Hemodynamic response curves extracted from automated box ROI centered at (±12, 12, 12) (with size 7x7x7 voxels). Compared with controls, patients had reduced and delayed hemodynamic responses in the caudate during the attended tone.

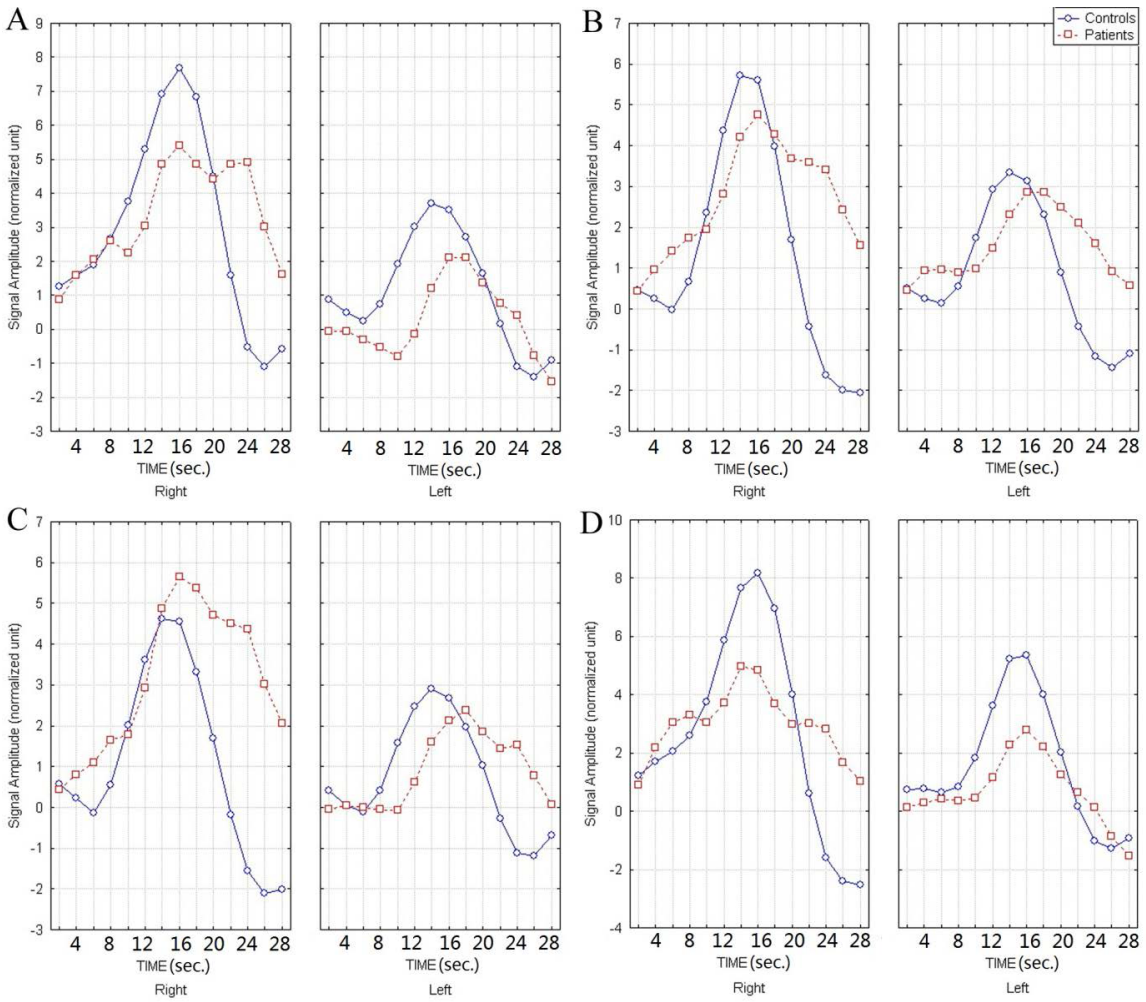

Figure 4: Hemodynamic response curves extracted from 4 pairs of automated box ROIs in the caudate.

A. Hemodynamic response curves extracted from a box ROI with center (±12, 12, 12)

B. Hemodynamic response curves extracted from a box ROI with center (±16, 12, 12)

C. Hemodynamic response curves extracted from a box ROI with center (±16, 16, 12)

D. Hemodynamic response curves extracted from a box ROI with center (±12, 8, 12)

Hemodynamic response curves extracted vary across different ROI hemispheres and locations.

centered at (± 12, 12, 12) has the highest correlation with the manual ROI which indicates that a larger automated box ROI when placed properly can be better correlated with the manual tracing.

The comparison of the hemodynamic response time course of the manual, semi-automated and automated ROI approaches shows that similar pattern of reduced and delayed hemodynamic responses in the caudate in the patients compared with the controls (Figure 3). The hemodynamic response time course extracted from the automated box ROIs indicates that (1) The shapes and amplitudes of the hemodynamic response curves extracted from the box-based ROIs are different between the left and right hemisphere (higher in right hemisphere); (2) The hemodynamic response curves vary from one ROI location to another which suggests that the location of the ROI box is critical to such automated ROI analysis (Figure 4).

Discussion

In this study, we compared the manual, semi-automated and automated ROI methods in extracting fMRI hemodynamic response time course in the caudate for schizophrenia patients and normal controls. We found that (1) schizophrenia patients have less activation with reduced hemodynamic response compared with controls (across the three ROI approaches); (2) The area under the hemodynamic response curves (AUCs) obtained from the manual and semi-automated approaches were highly correlated while large size automated box with appropriate location could generate AUC well-correlated with that of the manual approach. (3) The location and size of the automated box ROI is critical for the fMRI hemodynamic response curves extracted.

The first finding (reduced activations in the caudate nucleus in schizophrenia) is consistent with the findings in other fMRI studies in schizophrenia with tasks such as working memory and learning [4,12,15]. Since the structural and functional connectivity of various brain regions facilities brain function integration, activated brain regions with certain activation patterns may reflect the underlying

functional neural networks [25]. Since the caudate is linked with the frontal-striatal-thalamic circuitry, abnormal hemodynamic response in the caudate in patients with schizophrenia may reflect the functional deficits (e.g., attention impairment) in their frontal-striatal-thalamic circuitry. Such findings have been reported and further discussed by Hazlett et al. [17,26].

The rest of the findings in this study are related to the 3 ROI methods and all of them are based on anatomical ROIs. There are arguments on the weakness and strengths of anatomical ROIs vs. Functional ROIs (fROIs) in fMRI studies. In a pharmacological fMRI study [25,26], compared the anatomical and fROIs and found that the anatomical ROI (combined with an index of top 20% voxels of activation) was more reliable than the fROI approach in detecting the experimental effect [26]. In addition, they concluded that fROIs should be used with caution because the use of fROIs from individual sessions introduced unacceptable biases in the results, while the use of union fROIs yielded a lower sensitivity than anatomical ROIs [26,27]. However, when studying resting-state fMRI with functional connectivity measures and introducing a data-driven method for generating an ROI atlas by parcellating whole brain resting-state fMRI data into spatially coherent regions of homogeneous functional connectivity, Craddock et al. [28] found that the evaluated anatomical atlases showed poor ROI homogeneity which failed to reproduce functional connectivity results accurately [27]. These studies indicate that it may be appropriate to use anatomical ROIs for fMRI studies on hemodynamic response and activation, and use fROIs for studies on functional connectivity.

Despite the obvious differences in shape, size and different registration space between the manual and semi-automated ROI approaches, the two methods had significantly high ($p<0.05$) correlations, and detected smaller AUC of fMRI hemodynamic response in schizophrenia patients than controls (with RMS measurement), which suggests that the two methods extract similar time course from the fMRI data. However, there was relatively low correlation in the AUC between hand-traced ROI and box-based ROI (x12y12) with size 7×7×7 voxels and significant group difference for the box-based ROI. This can be explained by comparing the ROI locations in Figure 1 and the activated regions in the caudate in Figure 2 (SPM with contrast for effect of control - patient at group level). Figure 2 reveals that the differences in BOLD activations between control and patient groups are not uniformly distributed within the caudate which may be caused by the non-uniform BOLD signal distribution in the caudate of both groups. Since the box-based ROIs are located in the caudate regions which cover more significantly activated voxels, while the hand-traced ROI contains the whole caudate volume including the insignificantly activated regions, the time course extracted from these box-based ROIs reflected the averaged fMRI hemodynamic response of most significantly activated voxels within the ROI, while the time course extracted from the hand-traced ROI reflected an average of the hemodynamic response of mostly insignificantly activated voxels. Therefore, the averaged BOLD signal was stronger (i.e., the differences of BOLD signal between controls and patients are bigger) in these automated box-based ROIs than that of manual (hand-traced) ROI and such box-based ROIs are more sensitive in detecting group differences than manual ROI in group t-test. The non-uniformity of activation may also explain why the averaged signal amplitudes of fMRI hemodynamic response for all subjects are higher from the automated box ROIs than from the manual ROI.

In fMRI ROI analysis, one difficulty is how to measure fMRI signal within the ROI [28]. The program used in this study averages the BOLD responses of the voxels within the ROI and averaging them across all cycles. The practice of averaging responses over voxels across the entire region has the advantages in simplifying analyses and summarizing subject-specific responses without assuming anatomical homology over subjects. On the other hand, it is based on the assumption of functional homogeneity across the ROI and fMRI signals across voxels in the ROI may be functionally heterogeneous (activated or deactivated) [29]. The approach used in this study has weakness in dealing with heterogeneous BOLD responses across the ROI and could cancel out the BOLD responses of voxels with activation and deactivation within the ROI. In addition, it ignores the variations of various time course cycles. Consequently, bias may be introduced into this study. Rather than calculating the mean values, the latest version of SPM extracts the eigenvariate values in a region because eigenvariate values are more robust to heterogeneity of response within the ROI. Another fMRI ROI analysis software FSL-ROI toolbox extracts time courses for each condition at each voxel of the ROI using a finite impulse response (FIR) model. In the SPM and FSL ROI tools, the time courses extracted are not averaged across all trials. Such ROI time course extraction approaches are more advantageous and robust, which needs to be explored in our future studies.

Taken together, fMRI studies have revealed apparent functional anomalies in a number of brain disorders [13,30,31]. The possibility of detecting early signs of mental illness with non-invasive fMRI is promising to clinicians and patients. The potential for functional neuroimaging such as fMRI to elucidate brain responses and connectivity may ultimately contribute to clinical practice [32]. Toward that end, methodological exploration and advances in functional neuroimaging (especially fMRI) may release it from unreliability, inaccuracy and inefficiency, and help reach its full potential in clinical settings.

Conclusions

In summary, we investigated abnormalities of fMRI Hemodynamic Response (HR) in the caudate nucleus in schizophrenia with manual, semi-automated and automated approaches. Compared with controls, less activation (with weak and delayed fMRI HR) in the caudate was observed in the patient group with all of the 3 approaches. High correlations of the AUC were found between the manual and semi-automated ROI approaches, but not between the manual and the automated ROI approach. In addition, the location and size of the automated box ROI are critical for the fMRI hemodynamic response curve extracted, e.g., a larger box-ROI is slightly more highly correlated with the manual tracing. The abnormal fMRI hemodynamic response in the caudate in the patient group may suggest functional deficits in the frontal-striatal-thalamic circuit in schizophrenia. To speed up fMRI data analysis in anatomical ROI, the semi-automated approach may be used as an alternative to the manual approach in detecting fMRI experimental effect.

Acknowledgement

We are grateful for the cooperation of Department of Radiology at the Mt. Sinai Medical Center. This work is partly supported by NIH grant MH60023, and the Natural Science Foundation of China (Grant No. 81071211).

References

1. Ogawa S, Lee TM, Kay AR, Tank DW (1990) Brain magnetic resonance imaging with contrast dependent on blood oxygenation. Proc Natl Acad Sci U S A 87: 9868-9872.

2. Barkataki I, Kumari V, Das M, Sumich A, Taylor P, et al. (2008) Neural correlates of deficient response inhibition in mentally disordered violent individuals. Behav Sci Law 26: 51-64.

3. Hall J, Whalley HC, McKirdy JW, Romaniuk L, McGonigle D, et al. (2008) Overactivation of fear systems to neutral faces in schizophrenia. Biol Psychiatry 64: 70-73.

4. Koch, K, Wagner, G, Nenadic, I, Schachtzabel, C, Schultz, C, Roebel, M, Reichenbach, JR, Sauer, H, Schlösser, RG. (2008) Fronto-striatal hypoactivation during correct information retrieval in patients with schizophrenia: An fMRI study. Neuroscience.

5. McGuire P, Howes OD, Stone J, Fusar-Poli P (2008) Functional neuroimaging in schizophrenia: diagnosis and drug discovery. Trends Pharmacol Sci 29: 91-98.

6. Michalopoulou PG, Surguladze S, Morley LA, Giampietro VP, Murray RM, et al. (2008) Facial fear processing and psychotic symptoms in schizophrenia: functional magnetic resonance imaging study. Br J Psychiatry 192: 191-196.

7. Vinogradov S, Luks TL, Schulman BJ, Simpson GV (2008) Deficit in a neural correlate of reality monitoring in schizophrenia patients. Cereb Cortex 18: 2532-2539.

8. Hsu DT, Langenecker SA, Kennedy SE, Zubieta JK, Heitzeg MM (2010) fMRI BOLD responses to negative stimuli in the prefrontal cortex are dependent on levels of recent negative life stress in major depressive disorder. Psychiatry Res 183: 202-208.

9. Hashimoto R, Backer KC, Tassone F, Hagerman RJ, Rivera SM. (2011). An fMRI Study of the Prefrontal Activity during the Performance of a Working Memory Task in Premutation Carriers of the Fragile X Mental Retardation 1 Gene With and Without Fragile X-Associated Tremor/Ataxia Syndrome (FXTAS). J Psychiatr Res. 45, 36–43

10. Lopez AD, Murray CC (1998) The global burden of disease, 1990-2020. Nat Med 4: 1241-1243.

11. McGuire PK, Matsumoto K (2004) Functional neuroimaging in mental disorders. World Psychiatry 3: 6-11.

12. Carter CS, MacDonald AW 3rd, Ross LL, Stenger VA (2001) Anterior cingulate cortex activity and impaired self-monitoring of performance in patients with schizophrenia: an event-related fMRI study. Am J Psychiatry 158: 1423-1428.

13. Ford JM, Johnson MB, Whitfield SL, Faustman WO, Mathalon DH (2005) Delayed hemodynamic responses in schizophrenia. Neuroimage 26: 922-931.

14. Callicott JH, Egan MF, Mattay VS, Bertolino A, Bone AD, et al. (2003) Abnormal fMRI response of the dorsolateral prefrontal cortex in cognitively intact siblings of patients with schizophrenia. Am J Psychiatry 160: 709-719.

15. Whalley HC, Simonotto E, Flett S, Marshall I, Ebmeier KP, et al. (2004) fMRI correlates of state and trait effects in subjects at genetically enhanced risk of schizophrenia. Brain 127: 478-490.

16. Volz HP, Nenadic I, Gaser C, Rammsayer T, Häger F, et al. (2001) Time estimation in schizophrenia: an fMRI study at adjusted levels of difficulty. Neuroreport 12: 313-316.

17. Hazlett EA, Buchsbaum MS, Zhang J, Newmark R, Glanton, CF, et al. (2008). Schizophrenia-spectrum abnormalities in frontal-striatal-mediodorsal activation during a fMRI attention-to-prepulse startle paradigm. NeuroImage 42: 1164-1177.

18. Vink M, Ramsey NF, Raemaekers M, Kahn RS (2006) Striatal dysfunction in schizophrenia and unaffected relatives. Biol Psychiatry 60: 32-39.

19. Poldrack RA (2007) Region of interest analysis for fMRI. Soc Cogn Affect Neurosci 2: 67-70.

20. Fischl B, Salat DH, Busa E, Albert M, Dieterich M, et al. (2002) Whole brain segmentation: automated labeling of neuroanatomical structures in the human brain. Neuron 33: 341-355.

21. Fischl B, van der Kouwe A, Destrieux C, Halgren E, Ségonne F, et al. (2004) Automatically parcellating the human cerebral cortex. Cereb Cortex 14: 11-22.

22. Dade LA, Gao FQ, Kovacevic N, Roy P, Rockel C, et al. (2004) Semiautomatic brain region extraction: a method of parcellating brain regions from structural magnetic resonance images. Neuroimage 22: 1492-1502.

23. Talairach J and Tournoux P (1988). Co-Planar Stereotaxic Atlas of the Human Brain, Thieme Medical, New York.

24. Yushkevich PA, Piven J, Hazlett HC, Smith RG, Ho S, et al. (2006) User-guided 3D active contour segmentation of anatomical structures: significantly improved efficiency and reliability. Neuroimage 31: 1116-1128.

25. Smith SM, Jenkinson M, Woolrich MW, Beckmann CF, Behrens TE, et al. (2004) Advances in functional and structural MR image analysis and implementation as FSL. Neuroimage 23 Suppl 1: S208-219.

26. Hazlett EA, Buchsbaum MS, Tang CY, Fleischman MB, Wei TC, et al. (2001) Thalamic activation during an attention-to-prepulse startle modification paradigm: a functional MRI study. Biol Psychiatry 50: 281-291.

27. Mitsis GD, Iannetti GD, Smart TS, Tracey I, Wise RG (2008) Regions of interest analysis in pharmacological fMRI: how do the definition criteria influence the inferred result? Neuroimage 40: 121-132.

28. Craddock RC, James GA, Holtzheimer PE 3rd, Hu XP, Mayberg HS (2012) A whole brain fMRI atlas generated via spatially constrained spectral clustering. Hum Brain Mapp 33: 1914-1928.

29. Friston KJ, Rotshtein P, Geng JJ, Sterzer P, Henson RN (2006) A critique of functional localisers. Neuroimage 30: 1077-1087.

30. Schneider F, Weiss U, Kessler C, Müller-Gärtner HW, Posse S, et al. (1999) Subcortical correlates of differential classical conditioning of aversive emotional reactions in social phobia. Biol Psychiatry 45: 863-871.

31. Williamson P (2007) Are anticorrelated networks in the brain relevant to schizophrenia? Schizophr Bull 33: 994-1003.

32. Fletcher PC (2004) Functional neuroimaging of psychiatric disorders: exploring hidden behaviour. Psychol Med 34: 577-581.